INSTITUTE OF PHYSICS PUBLISHING NANOTECHNOLOGY
Nanotechnology **14** (2003) 778–785 PII: S0957-4484(03)60166-2

Small Ti clusters for catalysis of hydrogen exchange in $NaAlH_4$

Maximilian Fichtner[1,3], **Olaf Fuhr**[1], **Oliver Kircher**[1] **and Jörg Rothe**[2]

[1] Institute of Nanotechnology, Karlsruhe Research Centre, D-76021 Karlsruhe, Germany
[2] Institute for Nuclear Waste Management, Karlsruhe Research Centre, D-76021 Karlsruhe, Germany

E-mail: fichtner@int.fzk.de

Received 18 February 2003, in final form 11 April 2003
Published 13 May 2003
Online at stacks.iop.org/Nano/14/778

Abstract
Colloidal Ti has been synthesized following a method described in the literature. Extended x-ray absorption fine structure measurements indicate the presence of small colloidal entities, consisting of only a few core Ti atoms which are coordinated by O atoms from tetrahydrofuran (THF). The results can be explained by the proposed structure of Ti_{13}·6THF, in which the Ti cluster has the shape of a distorted icosahedron. The Ti colloid was used to prepare a functional nanocomposite by ball-milling the clusters with $NaAlH_4$. The nanocomposite showed superior hydrogen exchange kinetics when compared to the state of the art in the literature.

1. Introduction

For reversible storage of hydrogen in mobile applications, high pressure tanks, storage of liquid hydrogen at cryogenic temperatures and hydrogen storage in solid materials have been proposed. Although the latter seems to have several advantages [1], so far no reversible hydride system has been found which releases and again absorbs enough hydrogen at ambient temperatures and pressures within an adequate time.

Sodium alanate, $NaAlH_4$, is a complex metal hydride [2] which has been widely used for hydrogenation and reduction purposes, e.g., in organic syntheses. The reloading of the once decomposed hydride with hydrogen is possible, but the process is slow and occurs only under high pressures and at elevated temperatures [3] because the hydrogen exchange in the pure substance is kinetically hindered.

From the theoretical content of 7.5 wt% H, 5.6 wt% should be available from the reversible decomposition reactions (1) and (2). The third step, the decomposition of NaH (3), occurs at temperatures above 400 °C which is considered too high for most technical applications.

$$NaAlH_4 \leftrightarrows 1/3Na_3AlH_6 + 2/3Al + H_2 \quad (1)$$

$$1/3Na_3AlH_6 \leftrightarrows NaH + 1/3Al + 1/2H_2 \quad (2)$$

$$NaH \leftrightarrows Na + 1/2H_2. \quad (3)$$

[3] Author to whom any correspondence should be addressed.

In 1997 it was discovered that the kinetic barriers for the hydrogen uptake of the material can be lowered considerably when a transition metal promoter is added to the alanate [4]. The first attempts to introduce the catalyst were made using wet impregnation techniques with Ti tetra-n-butylate ($Ti(BuO)_4$) and Fe ethylate ($Fe(OEt)_2$), dissolved in toluene and diethylether. Numerous other materials including rare earth compounds were also investigated [5]. In this work, the influence of a bimetallic catalyst (Ti + Fe) was also studied. The precursor compounds were found to be reduced to metal particles by the hydride. From Mössbauer spectra, it was concluded that the size of the Fe particles was in the lower nanometre range. The reversible amount of hydrogen was about 4 wt% in these experiments.

Besides wet impregnation, the catalyst can also be incorporated by adding the precursor to the alanate and ball-milling the mixture under inert conditions [6, 7]. This technique was applied in screening experiments with many elements and confirmed early results which had indicated that Ti based promoters are most active for the hydrogen exchange [3, 8, 9]. Furthermore, it was shown in cycling experiments that dehydrogenated sodium alanate can be reloaded to 80% within about 35 min, at 125 °C and 91 bar hydrogen, when 2 mol% of $TiCl_3$ are added to $NaAlH_4$ and the mixture is treated in a ball mill under inert conditions [8].

However, there have so far been only a few attempts to investigate the role and nature of the Ti catalyst. From the

current state in the literature it is still an open question whether the Ti is active in a finely dispersed form at the surface of the hydride, whether it substitutes atoms in the alanate lattice, or whether both states contribute to the catalytic effect.

In one work, a lattice contraction of the alanate was detected after a mixture of $NaAlH_4$ and $TiCl_3$ had been treated in a ball mill and the associated lattice distortion was held responsible for the catalytic effect [10]. The distortion was explained by a substitution of Na^+ ions by variable valence Ti cations which created Na^+ vacancies in the lattice. However, these findings were not confirmed by other researchers [11], and it was also reported [4, 12] that at least some of the Ti stays at the surface of the alanate, where it may chemisorb hydrogen and enable its transfer to the hydride, across the grain boundaries. Furthermore, there are indications in the literature that carbon based impurities in the alanate lattice may also enhance the hydrogen exchange [3, 13], an effect which was attributed to a 'chemical modification' and destabilization of the alanate.

Another open question is whether there is a preferred size of the Ti particles. Changing the size of the particles may have an effect on the reaction rate irrespective of whether or not a mechanism similar to a heterogeneously catalysed hydrogenation at the surface of the hydride or a lattice alteration in the bulk occurs.

For heterogeneously catalysed reactions it is known that variations in the particle size may lead to changes in the catalytic activity [14]. The total reaction rate r at a carrier supported metal particle in contact with the gas phase may be expressed by

$$r \propto \mathrm{TOF} \times D \tag{4}$$

where TOF, the turnover frequency, is defined as the number of formed product molecules per exposed surface metal atom and per unit time. D stands for the fraction of exposed metal atoms of the catalyst [15], sometimes termed as dispersion.

Decreasing the particle size would increase the fraction of exposed metal atoms and therefore increase the reaction rate. In most cases, TOF itself is a function of the particle size and therefore structure sensitive. Electronic and/or geometric effects are held responsible for this behaviour and it was shown, for example, that dissociation of an adsorbing gas molecule may be enhanced if the cluster's HOMO (highest occupied molecular orbital) is close to the antibonding state of the molecule [16–18]. However, in the limit of atomic dispersion ($D = 1$), the discrete levels associated with an isolated atom prevail, which may prevent the catalytic effect.

If the catalytic effect is due to lattice contractions caused by atomic dispersed Ti and vacancies in the material, a higher dispersion of the Ti promoter may also lead to an increased reaction rate. As the diffusion of Ti into the lattice and substitution of Na is believed to be enhanced by the ball milling procedure, similar to mechanical alloying [10], a better coverage of the alanate particles with more finely dispersed Ti should promote the process because of the larger catalyst–hydride interface area and the shorter diffusion paths of the Ti into the lattice.

The aim of this work was to synthesize a highly dispersed Ti catalyst and to investigate its properties, since in the lower nanometre range many clusters show strongly size-dependent chemical and physical properties. Therefore, colloidal Ti clusters consisting of only a few atoms were synthesized,

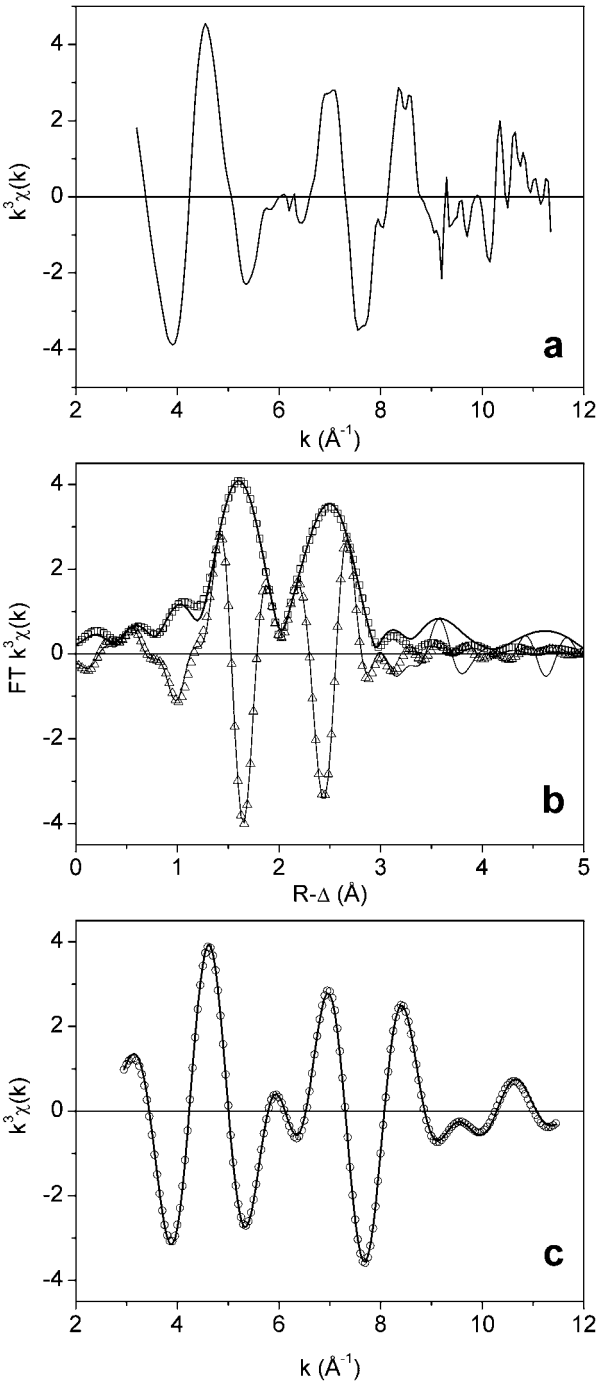

Figure 1. (a) k^3-weighted Ti K EXAFS $\chi(k)$-function of the unoxidized colloid sample; (b) FT magnitude (——) and imaginary part (–), R-space fit magnitude (□) and imaginary part (△); (c) Fourier filtered data and fit in k-space.

and the composition and structural properties examined and applied to the hydrogenation and dehydrogenation of $NaAlH_4$.

2. Experimental details

All sample preparations were done in an argon-filled glove box equipped with a recirculation system to keep the water

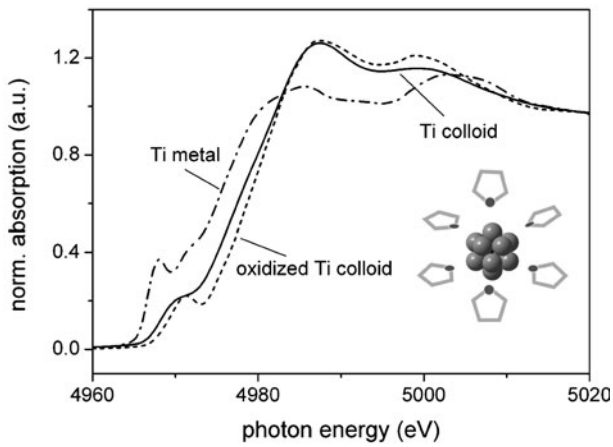

Figure 2. Normalized Ti K XANES of the unoxidized colloid sample, an oxidized colloid sample and a 5 μm Ti metal foil. The inset shows a sketch of the Ti cluster with six THF ligands and an icosahedral metal core.

and oxygen concentrations below 1 ppm during operation. Chemical synthesis was performed on the bench under purified N_2 using Schlenk tube techniques.

2.1. Reagents

Tetrahydrofuran (THF), diethylether and pentane (all Merck, p.A.) were distilled over sodium before use. $TiCl_3$ (99.999%, Sigma Aldrich), $TiBr_4$ (99.8%, Sigma Aldrich) and $KHBEt_3$ (1.0 M solution in THF, Sigma Aldrich) were used as received.

$NaAlH_4$ was obtained from a black and finely powdered technical product (Chemetall, Frankfurt). The material (100 g) was purified by a Soxhlet extraction with 500 ml THF. Some 400 ml of THF were drawn off slowly under vacuum, and large colourless crystals of $NaAlH_4$ (size about 0.5 mm) were obtained from the extract. The crystals were washed with dry diethylether and dried at ambient temperature under vacuum until a residual pressure of 1×10^{-3} mbar was reached.

An XRD analysis of the crystals showed a pattern which consisted of the same signals as pattern No 730088 from the JCPDS-ICDD powder diffraction data bank. No contributions from other compounds were detected. According to elemental analysis the purified $NaAlH_4$ contained 7.7 ± 0.1 wt% H and 0.2 ± 0.1 wt% C. Thermovolumetric analyses of several ball-milled, $TiCl_3$-doped $NaAlH_4$ samples (milling time 30 min) at 200 °C sample temperature delivered a hydrogen content of 5.2 ± 0.1 wt% H (theory: 5.6 wt%) from the first two decomposition steps (1) and (2).

2.2. XRD and elemental analysis

Powder x-ray diffraction measurements were performed with a Philips X'Pert diffractometer (Cu Kα radiation, 2 kW, with an X'Celerator RTMS detector). Air sensitive powders were covered by mineral oil, spread, and measured on a Si single crystal. The software for data acquisition and evaluation was X'Pert 1.3e and ProFit 1.0c.

Elemental analysis of carbon and hydrogen of $NaAlH_4$ and the Ti clusters was performed by using a CE Instruments Flash EA 1112 Series analyser with helium as purge gas. The typical amount of sample was 4–6 mg. For calibration, benzoic acid and aspartic acid were used as standards. Control measurements were made before and after measuring the samples.

A Varian Liberty 150 ICP-AES spectrometer was used to determine the content of Ti, K and B with an accuracy of about $\pm 2\%$. The sample was a solution of 11.3 mg product of the Ti cluster synthesis in 50 ml 0.01 M HNO_3.

2.3. X-ray absorption measurements/EXAFS

The black synthesis product was ground in an agate mortar and spread as a thin layer (lateral dimensions about 1×2 cm) on the sticky side of a Ti-free adhesive tape made of polycarbonate. The material was covered with a second strip of the same tape, sticky side down. Care was taken to provide a powder-free border region of about 5 mm in order to prevent oxygen from reacting with the powder.

Ti K x-ray absorption spectra were recorded at the ANKA-XAS beamline, Forschungszentrum Karlsruhe, Germany. The ANKA storage ring was operated at 2.5 GeV electron energy and a mean electron current of 100 mA. All spectra were taken in transmission mode at room temperature. Three air-filled ionization chambers at ambient pressure were used as an intensity monitor, for simultaneous detection of the transmission signals of the colloid samples and a Ti metal reference for energy calibration. Thereby, the 1s energy of Ti (4966 eV) was assigned to the first inflection point in the spectrum of Ti metal. Spectra were recorded at 4 eV step-width in the pre-edge region (4900–4955 eV), 1 eV at the rising edge (4956–4995 eV), 2 eV above the edge (4996–5020 eV) and equidistant k-steps (0.05 Å^{-1}) in the extended x-ray absorption fine structure (EXAFS) region (5021–6000 eV). The x-ray monochromator, equipped with a pair of Si$\langle 111 \rangle$ crystals ($2d = 6.271$ Å), was operated in fixed-exit mode. The intensity of the monitor ionization chamber was held constant during each scan by detuning the parallel alignment of the reflecting crystal faces to ~70% of the maximum beam intensity, thereby reducing the harmonic radiation impinging onto the sample.

EXAFS data analysis was based on standard least-squares fitting techniques [19] using the UWXAFS program package [20]. The ionization energy, corresponding to the origin of the photoelectron wavenumber (E_0), was fixed at the position of the first inflection point of the Ti metal K absorption edge. To extract the EXAFS $\chi(k)$-function, an atomic background ($\mu_0(E)$) was optimized with respect to spurious contributions below 1 Å in the Fourier transform (FT) of the data, using the '*autobk*' utility. Metric parameters of the atomic arrangement around the Ti absorber atoms (i.e., neighbour distances R_i, coordination numbers N_i and EXAFS Debye–Waller factors σ_i^2) were determined by modelling the EXAFS function as implemented in the '*feffit*' code, based on single-scattering paths generated by *FEFF8* [23]. Fits were performed in R-space after Fourier transformation of the $\chi(k)$-function.

The k^3-weighted EXAFS function $\chi(k)$, extracted by '*autobk*', is shown in figure 1(a). The noise level in this spectrum limits the useful data range to $k_{max} \leqslant 11.5$ Å^{-1}. A higher cut-off value introduces difficulties in the determination

Table 1. Metric parameters obtained by two-shell least-squares fitting analysis of EXAFS data taken from the unoxidized colloid sample (S_0^2 fixed at 1.0). Values in brackets represent parameters obtained in [22].

Backscatterer i	R-space fit range (Å)	R_i (Å) (±0.01 Å)	N_i (±0.2)	σ_i^2 (Å^2)	ΔE_i (eV)	Goodness of fit (%)
	1.23–2.95					0.3
O		2.02 (1.96)	1.4 (0.8)	0.004	10.5	
Ti		2.89 (2.83)	1.7 (1.8)	0.009	8.1	

of the atomic background function. The Fourier-transformed spectrum in figure 1(b) exhibits two intense FT peaks at about 1.6 and 2.5 Å ($R - \Delta$), corresponding to phase-shift-corrected values of about 2.0 and 2.9 Å, respectively. These resonances represent backscattering from the oxygen and titanium atoms comprising the first and second coordination spheres of Ti in the colloid sample. Table 1 summarizes the metric parameters obtained in the two-shell fit of the data performed in R-space. Fit results for the FT magnitude and the imaginary part are shown in figure 1(b); the corresponding back transformed (i.e., Fourier-filtered) data and k-space fit results are shown in figure 1(c).

To compare the near edge absorption (XANES) features in figure 2, spectra of the unoxidized sample used for EXAFS analysis, an oxidized sample and the Ti metal reference were normalized to the absorption edge-jump: a linear pre-edge background (4900–4950 eV) was subtracted, followed by averaging the first EXAFS oscillations (5000–5200 eV).

2.4. Volumetric measurements

For the hydrogenation/dehydrogenation experiments, all volumetric measurements were made in a carefully calibrated modified Sieverts apparatus (see figure 3), the components of which are made of stainless steel (316 and 316 l). Several calibrated gas reservoirs with different volumes, attached to a water bath, can be connected to the apparatus, resulting in an accessible volume for absorption and desorption measurements ranging from 25 to 2035 ml. Hydrogen pressures of up to 200 bar can be applied to the apparatus and its values are monitored using piezoresistive pressure transducers (Keller A G; pressure range 0–100 bar, error ±0.05% full scale; 100–200 bar, error ±0.03% full scale). To enhance the resolution for small pressure changes a differential pressure transducer between two distinct volume sections in the apparatus can be used. Samples are heated in a stainless steel reactor similar to the one described in [21] using an oil bath as heat reservoir in a temperature range from 0 up to 200 °C. Typical sample amounts of 1.5–2 g $NaAlH_4$ were located in a cylindrical slit with a width of only 1.25 mm to provide good heat exchange between the bath and the whole sample. A fast reacting thermocouple of 0.5 mm in diameter was in direct contact with the samples. Gas exchange with the Sieverts apparatus was possible via the inner tube being a porous sinter metal filter.

Desorption measurements were performed with the reactor connected to a large volume (≅1880 ml) of the Sieverts apparatus to prevent an interfering pressure increase, the pressure ranging typically between 0 and 0.5 bar. All desorption experiments were done at 150 °C sample temperature. Prior to the experiment the oil bath was elevated and the reactor submerged. Due to the endothermic reaction and the limited heat transfer in the reactor it took some time for the sample to reach the bath temperature (about 2 min for the $TiCl_3$-catalysed and, due to the higher reaction rate, up to 7 min for the Ti-cluster-catalysed samples). However, a temperature of 145 °C was already reached at 80 s for the $TiCl_3$-catalysed samples and at about 220 s for the Ti-cluster-catalysed samples.

Table 2. Type and amount of dopant in the $NaAlH_4$ samples. The concentrations refer to the amount of Ti in the sample.

	Sample 1	Sample 2	Sample 3
Ti_{13}·6 THF (mol%)	0.9	1.8	—
$TiCl_3$ (mol%)	—	—	2

Absorption measurements were performed with a smaller volume of the Sieverts apparatus (≅550 ml or ≅745 ml). The samples were always held at 100 °C sufficiently long before applying a pressure of around 100 bar.

2.5. Preparation of samples for absorption/desorption measurements

Three different types of sample were investigated on their hydrogenation/dehydrogenation properties. Each sample was prepared by adding a certain amount of catalyst to $NaAlH_4$, see table 2, and a subsequent treatment of the mixture in a ball mill.

Mechanical mixing and activation of the samples was done by milling them in a Fritsch P6 planetary mixer/mill at 600 rpm. Both milling vial and balls are of silicon nitride. Taking sample amounts of about 2 g and utilizing two balls with diameter of 20 mm and eight balls with diameter of 10 mm, a ball to powder weight ratio of about 20:1 was employed. The vial was filled in the glove box under an argon atmosphere and sealed. Milling times were 30 min.

3. Results and discussion

Synthesis of small Ti clusters was carried out following a description given by Franke *et al* [22]. The composition of the product was determined by ICP-OES and elemental analysis. As high resolution TEM investigations showed that the Ti clusters in the colloid were too small to show structural details or to produce lattice fringes, structural investigations were performed by EXAFS measurements. Employing this method, the number, type and distances of neighbouring atoms could be determined. The results were compared to previously published data [22].

The catalytic properties of the colloid were tested for the hydrogenation and dehydrogenation of $NaAlH_4$. The

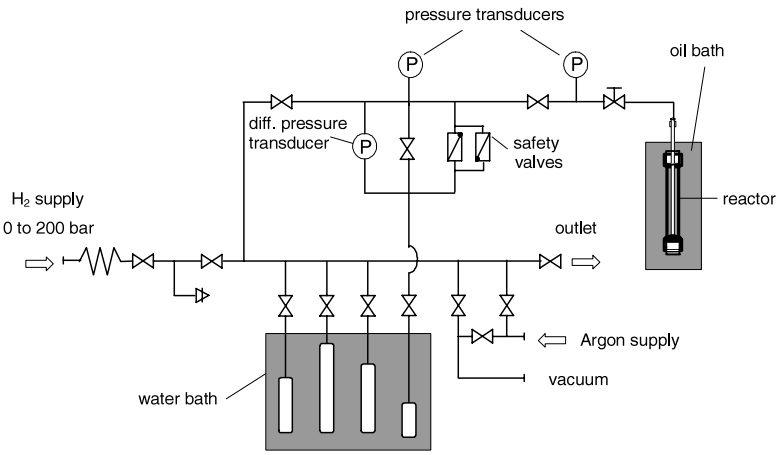

Figure 3. Experimental set-up for hydrogenation and dehydrogenation measurements of $NaAlH_4$. Gas reservoirs are attached to a water bath and the reactor is kept at constant temperature in an oil bath. The security valves are needed to protect the differential pressure transducer from overpressure.

Table 3. Amount of hydrogen absorbed in the first three absorption cycles for all three samples. The desorption values were determined after the respective absorption measurement.

Catalyst	Ti concentration (mol%)	Absorption no	wt% H_2 absorbed	wt% H_2 desorbed
$TiCl_3$	2	1	3.88	4.33
		2	3.95	4.28
		3	3.91	4.31
Ti_{13}·6 THF	1.8	1	3.91	4.75
		2	4.28	4.44
		3	4.52	4.53
Ti_{13}·6 THF	0.9	1	4.29	4.70
		2	4.28	4.47
		3	—	4.58

results of volumetric measurements in cycling experiments with Ti-cluster-catalysed and $TiCl_3$-catalysed hydride samples are compared and discussed.

3.1. Synthesis of $[Ti{\cdot}0.5THF]_x$

For the synthesis of the Ti clusters, 80 ml of a 1 M solution of $K[BEt_3H]$ in THF (0.08 mol) were added dropwise at −75 °C to a stirred suspension of $TiBr_4$·2THF (0.02 mol) in THF (1.5–2 h). After the addition was completed the suspension was allowed to warm up to room temperature and stirred for another 2 h. According to [22], the following reaction takes place:

$$TiBr_4{\cdot}2THF + 4K[BEt_3H] \rightarrow [Ti{\cdot}0.5THF]_x + 4BEt_3 + 4KBr \downarrow + 2H_2 \uparrow. \quad (5)$$

The dark grey suspension was stirred and cooled to −78 °C for 4 h. Then, the KBr was removed by filtering and the solvent was removed from the filtrate under vacuum. The black residue was extracted with 100 ml THF, filtered and the filtrate reduced to about 20 ml under vacuum. After adding 100 ml of dry pentane to the filtrate, the product precipitated as a black residue which was removed by filtering. It was dried under vacuum for several hours until a pressure of 2×10^{-3} mbar was reached.

The product was 1.65 g of a highly pyrophoric black powder which immediately went white when exposed to air. According to elemental analysis and ICP-OES it contained 25.4% Ti, 5.8% B, 5% K, 36.2% C and 7.5% H. The K content probably came from a residual amount of KBr in the product; the remaining percentage was attributed to O, which is contained in the THF. Assuming that Ti_{13}·6THF was the product species (see below), the powder contained about 43% of these clusters.

3.2. X-ray absorption measurements

The spectroscopic features near an inner shell x-ray absorption edge (XANES) represent electronic transitions from a core level into unoccupied electronic states, i.e., molecular orbitals or empty bands. From the presence, intensity and the energy position of distinct absorption features, information on the chemical state and the coordination geometry of the absorbing atoms can be derived. The analysis of the oscillatory fine structure of the absorption edges up to 1000 eV above the core electron binding energy, usually designated as the EXAFS $\chi(k)$-function [19], allows the determination of the average coordination environment of the absorbing atoms, i.e., their coordination numbers, type and distance of neighbour atoms and parameters characterizing pair distributions.

EXAFS function and metric parameters obtained from the unoxidized colloid sample were similar to those originally published for $[Ti^0{\cdot}0.5THF]_x$ in [22]. The characteristic two-shell structure with a rather short Ti–Ti distance (compared

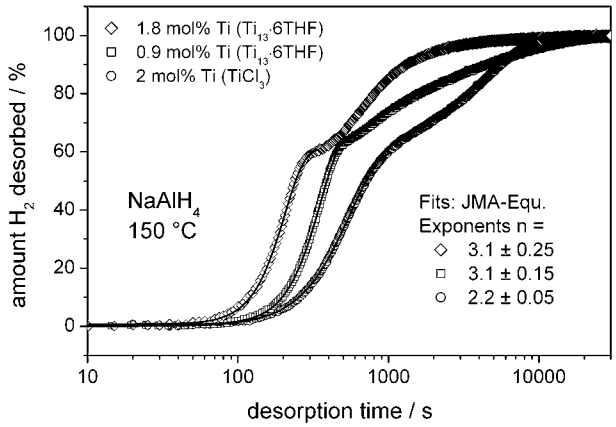

Figure 4. Dehydrogenation of samples 1–3 at 150 °C. The pressure rise during desorption never exceeded 0.5 bar. The two reaction steps according to equations (1) and (2) are clearly visible.

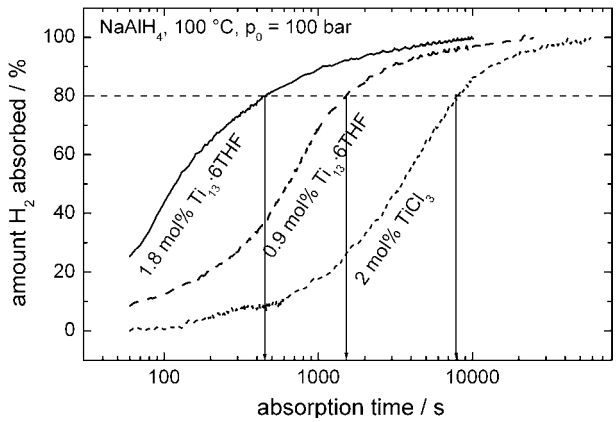

Figure 5. Hydrogenation of samples 1–3 at 100 °C. The applied pressure was 100 bar. The first 60 s are not shown due to equilibration after pressurizing the reactor (see text).

to the mean Ti bulk value of 2.92 Å), low Ti coordination number (∼2 Ti atoms in the second coordination sphere) and the absence of higher coordination shells (the small features at 3.5 and 4.5 Å ($R - \Delta$) must be attributed to noise) point again to the presence of small colloidal entities, consisting of only few core Ti atoms. The results are in accordance with the proposed structure of Ti_{13}·6THF.

The decrease of the N_{Ti}/N_O ratio in the present investigation to 1.2 (as compared to ∼2.3 found in [22]) indicates a significantly higher amount of oxygen interacting with the core metal atoms. This may be due to a different stoichiometric ratio of Ti atoms to THF molecules, or, more likely, to a higher permeability of our sample cell for oxygen during XAFS data acquisition. The increase of oxygen coordination is accompanied by a significant increase of the Ti–O and the Ti–Ti bond lengths by 2–3%. The high reactivity of the Ti colloids towards oxygen is emphasized by the comparison of the XANES features in figure 2. A colloid sample placed in the beam for several hours starts to develop the typical oxidation features described in [22] (edge-shift to higher energies, development of a pre-edge peak and intensity gain at the edge-crest region).

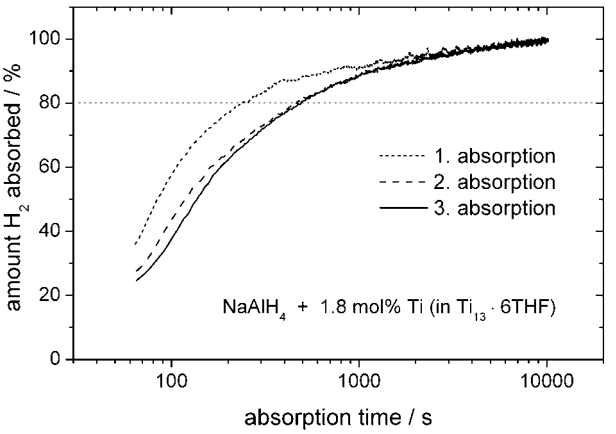

Figure 6. Hydrogenation curves of three subsequent absorption cycles for sample 2 (1.8 mol% Ti_{13}·6 THF). The experimental parameters correspond to those of figure 5.

3.3. Hydrogenation/dehydrogenation experiments

Figure 4 shows the amount of released hydrogen with desorption time for the third desorption cycle. For all samples a two-step desorption is observed according to equations (1) and (2). The shape of the curves gives clues for a nucleation and growth decomposition mechanism as the rate limiting step, which is typical for decomposition reactions of solids [24].

A clear shift of the desorption curves can be seen in figure 4. The release of hydrogen proceeds considerably faster for the materials with the Ti clusters as catalyst (samples 1 and 2) than for the $TiCl_3$-catalysed sample (sample 3) and it increases with increasing content of the Ti clusters. The time necessary to release 33% H, which is half of that released in the first decomposition step, was 190 and 310 s for samples 1 and 2 and 490 s for sample 3.

In a first analysis we fitted the first step of the desorption curves (ranging between 0 and 60 wt% H_2 desorbed) according to the Johnson–Mehl–Avrami (JMA) equation, describing transformations in metal hydrides driven by nucleation and growth [25]:

$$F = 1 - \exp\{-K(t - \tau)^{\eta}\}. \qquad (6)$$

Here, F denotes the converted fraction of the hydride, K the rate constant for thermal activation, t the time and τ an incubation time which was set to zero in our fits. The fits of curves 1 and 2 (see figure 4) show that η is about 3.1 and remains essentially the same when increasing the concentration of the Ti clusters, whereas the shift of the curves indicates a change in K. The difference from sample 3 where $\eta = 2.2 \pm 0.05$, can only be explained by alterations in K and η.

According to Rudman [26], the exponent η gives clues for the rate limiting processes and the dimensionality n of the growing phase of metal hydrides such as $LaNi_5$. A change in η could, for example, indicate a change of the growth dimensionality from $n = 2$ to 3 if the growth of the new phase is controlled by hydride–metal interface processes. In order to obtain experimental evidence of possible changes in the rate limiting step and/or in the growth dimensionality, further investigations are performed which will be presented in a forthcoming paper.

Four desorption measurements have been performed with each of the samples, recharging after each desorption measurement with an absorption cycle. We observed almost no change in the amount of desorbed hydrogen from the second to the fourth cycle. For both cluster compounds 4.6 ± 0.1 wt% and for the $TiCl_3$ compound 4.3 ± 0.1 wt% were released in each cycle (see table 3).

The data from the absorption measurements suffer from a larger experimental error due to the small relative changes of the pressure during the absorption step. Furthermore, the catalysed samples showed a pressure drop between the initial pressure (before opening the valve between the reactor and the remaining apparatus) and the pressure at the end of the equilibration phase about 1 min after opening the valve (the pressure change due to the change in volume was taken into account). This pressure drop was not observed with an empty reactor. As the absorbed amount of hydrogen was calculated starting with pressures at the end of the equilibration phase, there is a certain difference between the absorbed and the desorbed amount of hydrogen. The desorption measurements are, however, more accurate and are believed to be closer to the true values.

For the cluster-catalysed samples absorption was so rapid that the pressure drop due to initial absorption could not be accurately determined. Measurement with an empty reactor showed that it took around 50–60 s for pressure equilibration after applying 100 bar to the reactor and the gas reservoir (mainly due to the temperature difference between the apparatus and the reactor). To estimate the amount of hydrogen absorbed in the first 60 s we made short initial absorption measurements for 60–90 s, released the pressure and quantified the absorbed amount in a subsequent desorption. The results show that 0.3 wt% (sample 1) and 0.6 wt% (sample 2) hydrogen were absorbed in the first minute. Based on these results, the data in figure 5 were corrected accordingly.

Figure 5 shows absorption data for all samples. Like the desorption data the kinetics is much faster for the cluster-catalysed samples and increases with higher Ti content. The 80% value of the absorbed amount of hydrogen is reached about 20 times faster for sample 2 ($t_{80} = 460$ s) than for sample 3 ($t_{80} = 8000$ s). To our knowledge no catalyst has been presented in the literature enabling a faster kinetics for the absorption of hydrogen to form $NaAlH_4$.

With a 1.8 mol% Ti- (cluster-) doped sample we measured the trend of the kinetics during the first three absorption cycles. As can be seen from figure 6 the absorption rate in the first cycle was much faster than for the second one while the second and the third absorption proceeded almost at the same rate. Initially the second absorption was faster than the third, but after the 80% value no difference was observable between them. A gradual degradation or increase of the catalytic activity was therefore not observed in that early phase. However, in order to explore a possible aging behaviour of the catalyst, the system will need to be investigated in doing many more desorption and absorption cycles.

Because during the hydrogen uptake a distinct segregation between the reaction steps (1) and (2) could not be observed as for the desorption data, an analysis of the absorption curves presented in figure 5 was not performed. It is therefore intended to explore the absorption kinetics of the hydrogen uptake by separating the reaction steps (1) and (2), e.g. by a stepwise increase of the absorption pressures.

4. Conclusion

Small Ti clusters were successfully synthesized following instructions in the literature. The results of EXAFS measurements indicate a two-shell cluster with a Ti–Ti distance of 2.89 Å and a Ti–O distance of 2.02 Å. The value for the Ti–Ti bond is in accordance with bond lengths obtained with recent theoretical calculations for Ti_{13} clusters [26]. In this work, a distorted icosahedral structure was proposed for Ti_{13}, with a range of bond lengths between 2.52 and 2.98 Å. Such a structure could, in principle, explain the low coordination number of about 2 which was found in the evaluation of the EXAFS function. A sketch of a Ti cluster with six bound THF molecules is shown in the inset of figure 2. Franke *et al* [22] proposed that each THF O atom is coordinatively bound to three Ti atoms.

Compared to known catalysts for the hydrogen exchange with alanates, such as $TiCl_3$, the colloidal Ti exhibits the following outstanding features.

The theoretical amount of Ti in Ti_{13}·6THF (59% Ti) is much higher compared to other compounds such as $TiCl_3$ (31% Ti) or $Ti(BuO)_4$ (14% Ti). The hydrogenation and dehydrogenation measurements indicate, however, that the state of the precursor is of even greater importance than the simple amount of Ti in the material. The experiments show rather that the size of the Ti particles is crucial for the activity of the catalyst.

Effects associated with the small size of the Ti clusters seem to be responsible for the increase of the reaction rate when comparing it to $TiCl_3$-doped samples. According to equation (4), the increase is due to the very high dispersion of Ti_{13} which is about 0.92, and, possibly, other size related effects which may increase the turnover frequency. In order to separate these two factors it would be necessary to compare the catalytic activity of the small Ti clusters with those of other well defined Ti systems, e.g. larger clusters or particles, with a known value for the dispersion.

The apparent difference in the absorption data of our $TiCl_3$-doped samples ($t_{80} = 8000$ s) and the data presented by Gross *et al* [8] ($t_{80} = 2100$ s) may be explained as due to two factors. First, the samples in [8] were ball-milled for 3 h with 2 mol% of the catalyst, which is considerably longer compared to our milling times of 0.5 h. The longer milling times lead to a smaller particle size and a better mixing of the catalyst with the alanate. Second, our samples were measured at 100 °C compared to 125 °C in [8] where the absorption kinetics is faster.

From a technical aspect these first data of the Ti-cluster-doped samples are promising as it was shown that the refuelling times of alanate-based metal hydride tanks have come into the range of those of normal liquid fuels at gas stations. However, further work is necessary in order to investigate possible aging effects of the catalyst in long-term cycling experiments.

Acknowledgments

We are grateful for beam-time allotment by ANKA and experimental assistance by the ANKA-ISS staff. Harald Rösner is acknowledged for the TEM investigations, and Ralph Stahl at the ITC-CPV for the ICP-MS measurements.

References

[1] Schlapbach L and Züttel A 2001 *Nature* **414** 353–8
[2] Finholt A E, Bond A C and Schlesinger H I 1947 *J. Am. Chem. Soc.* **69** 1199
[3] Zaluska A, Zaluski L and Ström-Olsen J O 2000 *J. Alloys Compounds* **298** 125–34
[4] Bogdanovic B and Schwickardi M 1997 *J. Alloys Compounds* **253/254** 1–9
[5] Bogdanovic B, Brand R A, Marjanovic A, Schwickardi M and Tölle J 2000 *J. Alloys Compounds* **302** 36–52
[6] Zidan R A, Takara S, Hee A G and Jensen C M 1999 *J. Alloys Compounds* **285** 119–22
[7] Jensen C M and Gross K J 2001 *Appl. Phys.* A **72** 213–19
[8] Gross K J, Thomas G J and Jensen C M 2002 *J. Alloys Compounds* **330–332** 683–90
[9] Anton D L 2003 Catalytic effect of transition metal additions to $NaAlH_4$ for hydrogen desorption *Proc. Int. Symp. on Metal Hydrogen Systems (Annecy, France, Sept. 2002); J. Alloys Compounds* at press
[10] Sun D, Kiyobayashi T, Takeshita H T, Kuriyama N and Jensen C M 2002 *J. Alloys Compounds* **337** L8–11
[11] Bogdanovic B, Felderhoff M, Germann M, Hartel M, Pommerin A, Schuth F, Weidenthaler C and Zibrowius B 2003 *J. Alloys Compounds* **350** 246–55
[12] Gross K J, Guthrie S, Takara S and Thomas G 2000 *J. Alloys Compounds* **297** 270–81
[13] Dilts J A and Ashby E C 1972 *Inorg. Chem.* **11** 1230–6
[14] Che M and Bennett C O 1989 *Adv. Catal.* **36** 55–171
[15] Burwell R L 1977 *Adv. Catal.* **26** 351
[16] Heiz U, Sanchez A, Abbet S and Schneider W D 1999 *J. Am. Chem. Soc.* **121** 3214–17
[17] Heiz U, Vanolli F, Sanchez A and Schneider W D 1998 *J. Am. Chem. Soc.* **120** 9668–71
[18] Haruta M 1997 *Catal. Today* **36** 153–66
[19] Sayers D E and Bunker B A 1988 *X-Ray Absorption: Techniques of EXAFS, SEXAFS and XANES* ed D C Koningsberger and R Prins (New York: Wiley) pp 211–53
[20] Stern E A, Newville M, Ravel B, Yacoby Y and Haskel D 1995 *Physica* B **208/209** 117–20
[21] Friedlmeier G, Schaaf M and Groll M 1994 *Z. Phys. Chem.* **183** 185
[22] Franke R, Rothe J, Pollmann J, Hormes J, Boennemann H, Brijoux W and Hindenburg Th 1996 *J. Am. Chem. Soc.* **118** 12090–7
[23] Ankudinov A L, Ravel B, Rehr J J and Conradson S D 1998 *Phys. Rev.* B **58** 7565–76
[24] Bamford C H and Tipper C F H (ed) 1980 Comprehensive chemical kinetics *Reactions in the Solid State* vol 22 (Amsterdam: Elsevier)
[25] See, e.g., Christian J W 1961 *Transformations in Metals and Alloys* (Oxford: Pergamon) ch 12
[26] Rudman P S 1983 *J. Less-Common Met.* **89** 93–110
[27] Castro M, Liu S R and Wang L S 2003 *J. Chem. Phys.* **118** 2116–23